Antitumor activity of new hydridotris(pyrazolyl)borate ruthenium(II) complexes containing the phosphanes PTA and 1-CH_3–PTA†

Almudena García-Fernández,[a] Josefina Díez,[a] Ángel Manteca,[b] Jesús Sánchez,[b] Rósula García-Navas,[c,d] Beatriz G. Sierra,[c,d] Faustino Mollinedo,[c] M. Pilar Gamasa[a] and Elena Lastra*[a]

Received 25th March 2010, Accepted 12th August 2010
DOI: 10.1039/c0dt00206b

The synthesis and full characterization of new half-sandwich ruthenium(II) complexes containing $\kappa^3(N,N,N)$-hydridotris(pyrazolyl)borate ($\kappa^3(N,N,N)$-Tp) and the water-soluble phosphanes 1,3,5-triaza-7-phosphatricyclo[3.3.1.$1^{3,7}$]decane (PTA) and 1-methyl-3,5-diaza-1-azonia-7-phosphatricyclo[3.3.1.$1^{3,7}$]decane (1-CH_3-PTA) has been explored. Single crystal X-ray diffraction analysis for complex [RuCl{$\kappa^3(N,N,N)$-Tp}(PMe_2Ph)(1-CH_3-PTA)][CF_3SO_3]·2NCMe is also reported. DNA binding properties of the ruthenium complexes have been evaluated by mobility shift assay and MALDI-TOF mass spectrometry. The *in vitro* antitumor activity of these compounds was assessed by examining their ability to inhibit cell proliferation in a number of human cancer cell lines (NCI-H460, SF-268, MCF-7) and non-tumor human umbilical vein endothelial cells (HUVEC). Some of these new compounds show promising cytotoxic activity with IC_{50} values in the low micromolar range, and display differential effects on cancer and normal cell growth.

Introduction

Metal complexes that exhibit water solubility and the capacity to link to nucleobases, DNA fragments, amino acids, peptides, and proteins are currently receiving special attention mainly due to the clinical usefulness of transition metal complexes as antitumor drugs.[1–3]

Ruthenium-based anticancer drugs have been the subject of active research,[4–6] thanks to the fact that ruthenium(II) complexes represent an alternative to platinum antitumor drugs.[7,8] Thus, ruthenium complexes [ImH][*trans*-$RuCl_4$(Im)(DMSO)] (Im = Imidazole) NAMI-A, and complexes [ImH][*trans*-$RuCl_4(Im)_2$(DMSO)] KP1019 have already successfully completed Phase I clinical trials.[9–11] Ru(II) arene complexes have also shown excellent *in vitro* results revealing high selectivity and low general toxicity.[12–15]

One of the most common approaches to obtaining water-soluble organometallic compounds is by means of ligands with hydrophilic properties. Among water-soluble phosphanes, particular attention has recently been paid to the cage-like tertiary phosphane 1,3,5-triaza-7-phosphatricyclo[3.3.1.13,7]decane (PTA);[16] furthermore, complexes containing arene and PTA ligands (RAPTA complexes) have been extensively used in biological assays.[17–20]

Current interest in the design of new ruthenium complexes as therapeutic agents focuses on the role that arene and ancillary ligands play in determining the chemical properties and hence, biological activity of these complexes. Thus, recent studies on the anticancer activity of ruthenium arene complexes showed the relationship between the size of the arene and biological activity, cytotoxicity increasing with the size of the arene ring.[21,22]

Despite the many ruthenium-arene complexes tested as therapeutic agents, few attempts have been made to develop half-sandwich complexes other than arene complexes for this purpose. Thus, to the best of our knowledge, no studies have been performed with hydridotris(pyrazolyl)borate ruthenium(II) complexes and only a few have been found for ruthenium-cyclopentadienyl derivatives.[23–25]

Hydridotris(pyrazolyl)borate ligand[26,27] (Tp) is generally considered analogous to Cp due to the fact that it has the same charge and number of electrons donated even when a Tp cone angle close to 180° is well above the 100° and 146° calculated for Cp and Cp*, respectively. This increase in size might favour greater anticancer activity as previously described for ruthenium-arene derivatives.

In this context, we recently described the first examples of hydridotris(pyrazolyl)borate ruthenium(II) complexes containing the water-soluble PTA and 1-CH_3-PTA phosphane ligands and their interaction with plasmidic DNA by using a mobility shift assay.[28] Moreover, their antimicrobial activity was tested revealing that [RuX{$\kappa^3(N,N,N)$-Tp}(PPh_3)(1-Me-PTA)][CF_3SO_3] (X = Cl, H) complexes were quite active against prokaryotic microorganisms.

In this work, we present the synthesis and DNA-binding properties tested by shift mobility assays of new ruthenium compounds [RuCl{$\kappa^3(N,N,N)$-Tp}(L)(PTA)] (L = PMe_2Ph (**1c**), PMe_3 (**1d**), $P(OMe)_3$ (**1e**), $P(OPh)_3$ (**1f**)), [RuCl{$\kappa^3(N,N,N)$-Tp}(L)(1-CH_3-PTA)] (L = PMe_2Ph (**2c**), PMe_3 (**2d**), $P(OMe)_3$ (**2e**), $P(OPh)_3$

[a]*Departamento de Química Orgánica e Inorgánica, Instituto de Química Organometálica "Enrique Moles" (Unidad Asociada al C.S.I.C.). Universidad de Oviedo, 33006, Oviedo, Spain. E-mail: elb@uniovi.es; Fax: 34 985103446*
[b]*Área de Microbiología, Departamento de Biología Funcional, Instituto Universitario de Biotecnología de Asturias. Universidad de Oviedo, 33006, Oviedo, Spain*
[c]*Centro de Investigación del Cáncer, Instituto de Biología Molecular y Celular del Cáncer, CSIC-Universidad de Salamanca, Campus Miguel de Unamuno, E-37007, Salamanca, Spain*
[d]*APOINTECH, Centro Hispano-Luso de Investigaciones Agrarias (CIALE), Parque Científico de la Universidad de Salamanca, C/ Rio Duero 12, E-37185, Villamayor, Salamanca, Spain*

† Electronic supplementary information (ESI) available: The synthesis and characterization of complexes **1c–f** and **2c–f**. CCDC reference number 763580 (**2c**·2NCMe). For ESI and crystallographic data in CIF or other electronic format see DOI: 10.1039/c0dt00206b

Table 1 Ruthenium [Ru(Tp)(PTA)] complexes

L	PTA	PPh_3	PMe_2Ph	PMe_3	$P(OMe)_3$	$P(OPh)_3$
[RuCl(Tp)(L)(PTA)]	**1a**[a]	**1b**[a]	**1c**	**1d**	**1e**	**1f**
[RuCl(Tp)(L)(1-CH_3-PTA)][OTf]		**2b**[a]	**2c**	**2d**	**2e**	**2f**
[RuCl(Tp)(1-CH_3-PTA)$_2$][OTf]$_2$	**2a**[a]	[Ru(Tp)(NCMe)(PPh_3)(PTA)][PF_6]				**5′**[a]
[RuH(Tp)(PPh_3)(PTA)]	**3**[a]	[Ru(Tp)(NCMe)(PPh_3)(PTA)][OTf]				**5**
[RuH(Tp)(PPh_3)(1-CH_3-PTA)][OTf]	**4**[a]	[Ru(Tp)(NCMe)(PPh_3)(1-CH_3-PTA)][OTf]$_2$				**6**

[a] Synthesis, interaction with plasmidic DNA, and antimicrobial activity described in ref. 28.

(**2f**)), [Ru{κ³(*N*,*N*,*N*)-Tp}(NCMe)(PPh_3)(PTA)][CF_3SO_3] (**5**) and [Ru{κ³(*N*,*N*,*N*)-Tp}(NCMe)(PPh_3)(1-CH_3-PTA)][CF_3SO_3]$_2$ (**6**). Moreover, we go one step further in the characterization of these new complexes, as well as the ones previously reported (see Table 1), by evaluating their antitumor activity against three well characterized tumor cell lines (NCI-H460, SF-268, MCF-7). We also report toxicity data against non-tumor cells (HUVEC) in order to illustrate the possible therapeutic index of some of these compounds.

Results and discussion

Synthesis of complexes [RuCl{κ³(*N*,*N*,*N*)-Tp}(L)(PTA)] (L = PMe_2Ph (1c), PMe_3 (1d), $P(OMe)_3$ (1e), $P(OPh)_3$ (1f))

Complex [RuCl{κ³(*N*,*N*,*N*)-Tp}(PPh_3)(PTA)] (**1b**) reacts with an excess of the corresponding phosphane or phosphite to yield the complexes [RuCl{κ³(*N*,*N*,*N*)- Tp}(L)(PTA)] (L = PMe_2Ph (**1c**), PMe_3 (**1d**), $P(OMe)_3$ (**1e**), $P(OPh)_3$ (**1f**)), which were obtained as pale yellow (**1c**) or white solids in moderate yields (45–67%) (Scheme 1).

Complexes **1c–1f** show low water solubility (3–4 mg mL^{-1}) and are soluble in common organic solvents such as methanol, chloroform, and dichloromethane and insoluble in acetone, diethyl ether, and hexane. The complexes have been analytically and spectroscopically characterized (IR and ^1H, $^{13}C\{^1H\}$ and $^{31}P\{^1H\}$ NMR). In particular, it must be noted that: i) the IR spectra (KBr) show the characteristic ν(BH) absorption for the Tp ligand in the range 2462–2480 cm^{-1}; ii) $^{31}P\{^1H\}$ spectra exhibit the expected two doublets corresponding to the PTA ligand (–26.6 to –34.9 ppm) and to the other phosphorous ligand (21.1 ppm, $^2J_{CP}$ = 29 Hz (PMe_2Ph); 13.9 ppm, $^2J_{CP}$ = 39 Hz (PMe_3); 151.5 ppm, $^2J_{CP}$ = 64 Hz ($P(OMe)_3$); 128.7 ppm, $^2J_{CP}$ = 64 Hz ($P(OPh)_3$)); iii) the ^1H and $^{13}C\{^1H\}$ NMR spectra for all the complexes agree with the presence of the hydride trispyrazolylborate group, the PTA phosphane and the corresponding phosphorous donor ligand (See experimental).

Methylation reactions of complexes 1c–f: Synthesis of complexes [RuX{κ³(*N*,*N*,*N*)-Tp}(L)(1-CH_3-PTA)][CF_3SO_3] (L = PMe_2Ph (2c), PMe_3 (2d), $P(OMe)_3$ (2e), $P(OPh)_3$ (2f)). The treatment of the complexes **1c–f** with $MeCF_3SO_3$ in CH_2Cl_2 at –30 °C leads to the methylation of one of the nitrogen atoms of the PTA ligand, resulting in the complexes containing the 1-methyl-3,5-diaza-1-azonia-7-phosphaadamantane (1-CH_3-PTA) triflate ligand. The complexes [RuCl{κ³(*N*,*N*,*N*)-Tp}(L)(1-CH_3-PTA)][CF_3SO_3] (L = PMe_2Ph (**2c**), PMe_3 (**2d**), $P(OMe)_3$ (**2e**), $P(OPh)_3$ (**2f**)) have been isolated as white solids (Scheme 2) at a yield of 60–65%.

Water solubility of these complexes (1.5–3mg mL^{-1}) decreases with respect to the parent compounds. Conductivity measurements in acetonitrile for complexes **2c–2f** (116–141 S cm^2 mol^{-1}) are in the range to be expected for 1 : 1 electrolytes and elemental analysis and spectroscopic data are consistent with the proposed formulations. Thus, the phosphorous atom signal of the 1-CH_3-PTA ligand in the $^{31}P\{^1H\}$ NMR spectra (δ = –8.2 (**2c**), –6.7 (**2d**), –8.2 (**2e**), –10.0 (**2f**)) appears shifted at lower fields compared to the PTA ligand in the spectra of the former complexes as observed for previously synthesized complexes.[29] ^1H NMR and $^{13}C\{^1H\}$ NMR spectra agree with the proposed stoichiometry and display the peak corresponding to the methyl group in range 2.62–2.79 ppm (CH_3) and 48.9–49.0 ppm (CH_3).

Slow evaporation of the solvent in an NCMe solution of complex **2c** gives rise to suitable crystals for X-ray diffraction studies. The asymmetric unit consists of a [RuCl{κ³(*N*,*N*,*N*)-Tp}(L)(1-CH_3-PTA)$_2$][CF_3SO_3] molecule and two acetonitrile

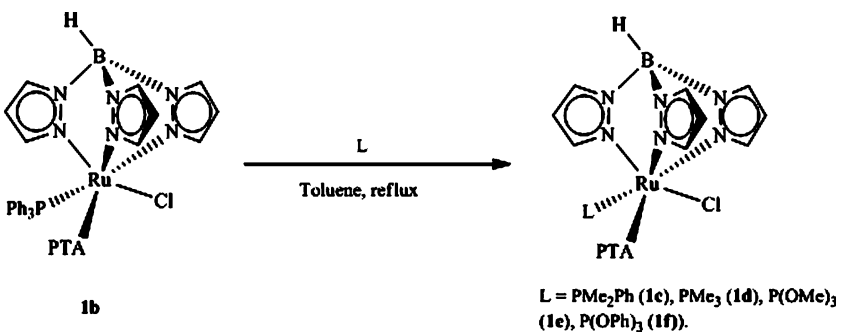

1b

L = PMe_2Ph (1c), PMe_3 (1d), $P(OMe)_3$ (1e), $P(OPh)_3$ (1f).

Scheme 1

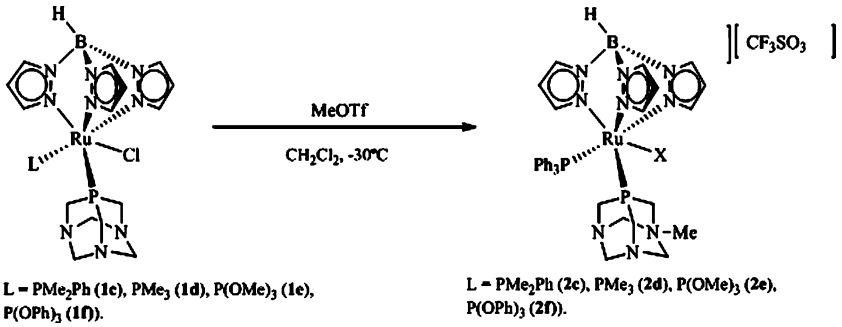

Scheme 2

molecules. An ORTEP type representation is shown in Fig. 1. Selected bonding data are presented in the caption.

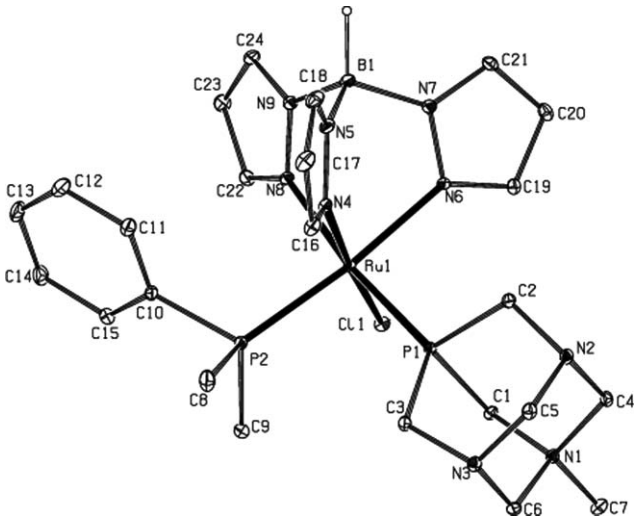

Fig. 1 Molecular structure and atom-labelling scheme for the cation of complex **2c**·2NCMe. Solvent molecules and hydrogen atoms, except for the B–H, have been omitted for clarity. Non hydrogen atoms are represented by their 10% probability ellipsoids. Selected bond lengths (Å): Ru(1)–N(4) = 2.085(2), Ru(1)–N(6) = 2.156(2), Ru(1)–N(8) = 2.143(2), Ru(1)–P(1) = 2.2662(7), Ru(1)–P(2) = 2.2959(8), Ru(1)–Cl(1) = 2.4327(7). Selected bond angles (°): N(4)–Ru(1)–N(8) = 89.08(9), N(4)–Ru(1)–N(6) = 86.46(9), N(8)–Ru(1)–N(6) = 81.68(9), N(4)–Ru(1)–P(1) = 91.25(7), N(8)–Ru(1)–P(2) = 94.03(7), N(6)–Ru(1)–P(1) = 90.97(6), N(4)–Ru(1)–P(2) = 94.03(7), N(8)–Ru(1)–P(2) = 91.34(7), N(6)–Ru(1)–P(2) = 172.99(6), N(4)–Ru(1)–Cl(1) = 174.67(7), N(8)–Ru(1)–Cl(1) = 87.29(7), N(6)–Ru(1)–Cl(1) = 89.15(6), P(1)–Ru(1)–Cl(1) = 91.84(3), P(2)–Ru(1)–Cl(1) = 89.96(3), P(1)–Ru(1)–P(2) = 96.01(3).

The ruthenium atom exhibits a distorted octahedral coordination geometry bonded $\kappa^3(N,N,N)$ to the hydridotris(pyrazolyl)borate ligand, to one chlorine atom, and to the phosphorous atoms of the 1-CH_3-PTA and PMe_2Ph ligands. The interligand N–Ru–N angles (81.68(9)–89.08(9)°) and Ru–N bond distances (Ru–N 2.085–2.156 Å) are in the range of those found for other divalent ruthenium complexes, such as [RuCl{$\kappa^3(N,N,N)$-Tp}(NCMe)(PPh_3)] (Ru–N 2.088–2.159 Å).[30] The Ru–N bond distances *trans* to the phosphane ligands (2.156(2) and 2.143(2) Å) are significantly longer than the Ru–N distances *trans* to the chlorine atom (Ru(1)–N(4) = 2.085(2) Å) according with the higher *trans* influence for the phosphane ligands.[31–33]

Synthesis of complexes [Ru{$\kappa^3(N,N,N)$-Tp}(NCMe)(PPh_3)(PTA)][CF_3SO_3] (5) and [Ru{$\kappa^3(N,N,N)$-Tp}(NCMe)(PPh_3)(1-CH_3-PTA)][CF_3SO_3]$_2$ (6). The heating of a solution of complex [RuCl{$\kappa^3(N,N,N)$-Tp}(PPh_3)(PTA)] in a mixture of acetonitrile–methanol (1 : 5) with sodium triflate renders the complex [Ru{$\kappa^3(N,N,N)$-Tp}(NCMe)(PPh_3)(PTA)][CF_3SO_3] (**5**), which was obtained at a 45% yield rate. The treatment of complex **5**, at −30 °C with $MeCF_3SO_3$ in CH_2Cl_2 leads to the methylation of one of the nitrogen atoms of the PTA ligand, resulting in the complex [Ru{$\kappa^3(N,N,N)$-Tp}(NCMe)(PPh_3)(1-CH_3-PTA)][CF_3SO_3]$_2$ (**6**).

Complexes **5** and **6** have been analytically and spectroscopically characterized (IR and ^{1}H, ^{13}C{^{1}H} and ^{31}P{^{1}H} NMR). In particular, it must be noted that: i) the IR spectra (KBr) exhibit the characteristic ν(BH) absorption for the Tp ligand at 2488 (**5**) and 2492 (**6**) cm^{-1} as well as the three characteristic absorptions for the CF_3SO_3 group in the range of 1264–1030 cm^{-1}; ii) ^{31}P{^{1}H} spectra exhibit the expected two doublets corresponding to the PPh_3 (44.2 ppm (**5**) and 39.7 ppm (**6**)) and the PTA (–42.5 ppm (**5**)) or 1-CH_3-PTA (–16.7 ppm (**6**)) ligands; iii) the ^{1}H and ^{13}C{^{1}H} NMR spectra agree with the proposed stoichiometry showing the presence of the trispyrazolylborate group, the corresponding phosphanes, and the acetonitrile group ((2.27 (**5**) and 2.25 (**6**) ppm (CH_3CN) and 126 (**5**) and 127,5 (**6**) ppm (CH_3CN)).

Despite the ionic character of both complexes, water solubility is rather low. As indicated for complexes **2c–f**, the water solubility of complex **6** (0.33 mg mL^{-1}) is lower than the parent complex **5** (1.30 mg mL^{-1}).

Electrochemical studies of ruthenium complexes. Electrochemical studies on selected complexes were carried out in order to establish relationships between the donor character of the ancillary ligands and the electrochemical behaviour of the complexes. Thus, cyclic voltammetry (CV) experiments in solutions 0.15M [Bu_4N][BF_4] in DMF were performed at a Pt electrode for complexes **1b,c,e**, **2b,c,e**, **3** and **4**. CV for the chloride complexes [RuCl{$\kappa^3(N,N,N)$-Tp}(L)(PTA)] (**1b,c,e**) and [RuCl{$\kappa^3(N,N,N)$-Tp}(L)(1-CH_3-PTA)][OTf] (**2b,c,e**) show a reversible one-electron oxidation wave[34] assigned to the Ru(II)/Ru(III) oxidation as shown in Table 2. The values of the Ru(II)/Ru(III) oxidation reflect the electron-donor character of the ligands, which can be ordered as expected 1-CH_3-PTA < PTA and $P(OMe)_3$ < PPh_3 < PMe_2Ph.

For the hydride complexes **3** and **4** CV experiments show an irreversible oxidation wave which can be caused for a chemical decomposition of the Ru(III) species.

Table 2 Cyclic voltammetric data[a] for [Ru(Tp)(PTA)] complexes

	$E^{\circ}_{1/2}$/V	E°_{ox}/V
[RuCl{κ³(*N*,*N*,*N*)-Tp}(PPh_3)(PTA)] (**1b**)	1.015	1.052
[RuCl{κ³(*N*,*N*,*N*)-Tp}(PMe_2Ph)(PTA)] (**1c**)	1.006	1.044
[RuCl{κ³(*N*,*N*,*N*)-Tp}{$P(OMe)_3$}(PTA)] (**1e**)	1.227	1.277
[RuCl{κ³(*N*,*N*,*N*)-Tp}(PPh_3)(1-CH_3-PTA)][OTf] (**2b**)	1.179	1.211
[RuCl{κ³(*N*,*N*,*N*)-Tp}(PMe_2Ph)(1-CH_3-PTA)][OTf] (**2c**)	1.139	1.183
[RuCl{κ³(*N*,*N*,*N*)-Tp}{$P(OMe)_3$}(1-CH_3-PTA)][OTf] (**2e**)	1.262	1.296
[RuH{κ³(*N*,*N*,*N*)-Tp}(PPh_3)(PTA)] (**3**)		0.727
[RuH{κ³(*N*,*N*,*N*)-Tp}(PPh_3)(1-CH_3-PTA)][OTf] (**4**)		0.904

[a] In DMF at a platinum-bead electrode. Under the conditions used the potential for $[Fe(\eta\text{-}C_5H_5)_2]^+$-$[Fe(\eta\text{-}C_5H_5)_2$ is 0.75 V.

DNA binding properties and cytotoxicity of ruthenium complexes. The plasmid DNA binding properties for the new complexes synthesized in this work (**1c–f**, **2c–f**, **5**, and **6**) were studied. To do so, we used the plasmidic DNA mobility shift assay previously reported.[28] Binding of ruthenium complexes to linear DNA does not produce enough of an increment in the molecular weight to be observed in an agarose gel; however, their interaction with circular DNA increases the proportions of the relaxed forms (open circular DNA). Different concentrations were used for each complex as a function of their solubility (see Methods). Changes in the plasmid DNA mobility were observed for all the analyzed complexes, being especially evident for compounds **1e**, **2c**, **2d**, **2e**, **5**, and **6** (Fig. 2). Interestingly, the most soluble compounds (**1d**, 3,8 mg mL^{-1} and **1f**, 4 mg mL^{-1}), those for which we have used the greatest concentrations, showed minor interaction with plasmidic DNA. By contrast, the most insoluble compounds (**2c**, 1,9 mg mL^{-1}; **2d**, 2,8 mg mL^{-1}; **2e**, 3 mg mL^{-1}; **5**, 1.3 mg mL^{-1} and **6**, 0.33 mg mL^{-1}) showed the greatest interactions. This could be suggesting some kind of mechanism in which hydrophobic compounds can interact with the hydrophobic core of the DNA molecule (the bases inside the double helix) destabilizing the secondary structure of the DNA, and increasing the plasmid relaxed forms. One exception was compound **2f**, which showed a low solubility (1,5 mg mL^{-1}) and a poor interaction with plasmidic DNA. Overall, the different patterns of DNA mobility observed between the different compounds (compare for instance compounds **2c** and **2e** with **1e**), could indicate different mechanisms of interaction since they can interact with different bases or even different regions inside the DNA. Much remains to be learned about DNA-ruthenium interactions, and further experiments will be necessary to define the specific DNA binding mechanisms of the ruthenium drugs.

DNA binding properties of ruthenium complexes analyzed by MALDI-TOF mass spectrometry. Interaction of the complexes [RuCl{κ³(*N*,*N*,*N*)-Tp}($PTA)_2$] (**1a**), [RuCl{κ³(*N*,*N*,N)-Tp}{$P(OMe)_3$}(PTA)] (**1e**), [RuCl{κ³(*N*,*N*,*N*)-Tp}(L)(1-CH_3-PTA)][CF_3SO_3] (L = PPh_3 (**2b**), PMe_2Ph (**2c**), PMe_3 (**2d**), $P(OMe)_3$ (**2e**)), [RuH{κ³(*N*,*N*,*N*)-Tp}(PPh_3)(PTA)] (**3**), and [RuH{κ³(*N*,*N*,*N*)-Tp}(PPh_3)(1-CH_3-PTA)][CF_3SO_3] (**4**), with the 14-mer single stranded oligonucleotide 5′ATACATGGTACATA 3′ was analyzed by MALDI-TOF mass spectrometry. The analyses of the mass spectra are consistent with the interaction of the drugs **2b**, **3**, and **4** with the oligonucleotide (See Table 3 and Fig. 3). For the rest of the complexes tested, while bonding to the oligonucleotide was not detected by MALDI-TOF mass spectrometry, their interaction with circular DNA was observed by shift mobility assays in agarose gels (see above and Fig. 2). Consequently, both techniques should be considered complementary. Thus, a negative result in the MALDI-TOF experiment does not exclude interaction with DNA, while a positive result proves DNA interaction.

For complexes **2b**, **3**, and **4** the *m*/*z* peaks detected were those related to the adducts of the oligonucleotide bonded to different fragments of each ruthenium complex. As illustrated in Table 3, the chloride anion is lost in all cases. In five of the six *m*/*z* peaks observed (Table 3, entries 1, 2, 4, 5 and 6), the fragments [Ru{κ³(*N*,*N*,*N*)-Tp}(PTA)] (entry 4) and [Ru{κ³(*N*,*N*,*N*)-Tp}(1-CH_3-PTA)] (entries 1, 3, and 5) are coordinated to the oligonucleotide, indicating the loss of the PPh_3 ligand.[35] Moreover, these three complexes also exhibit a strong interaction with the plasmidic DNA.[28]

These results suggest the coordination of the metal fragment [Ru{κ³(*N*,*N*,*N*)-Tp}(PTA)] or [Ru{κ³(*N*,*N*,*N*)-Tp}(1-CH_3-PTA)] to the oligonucleotide, supporting an action mechanism which

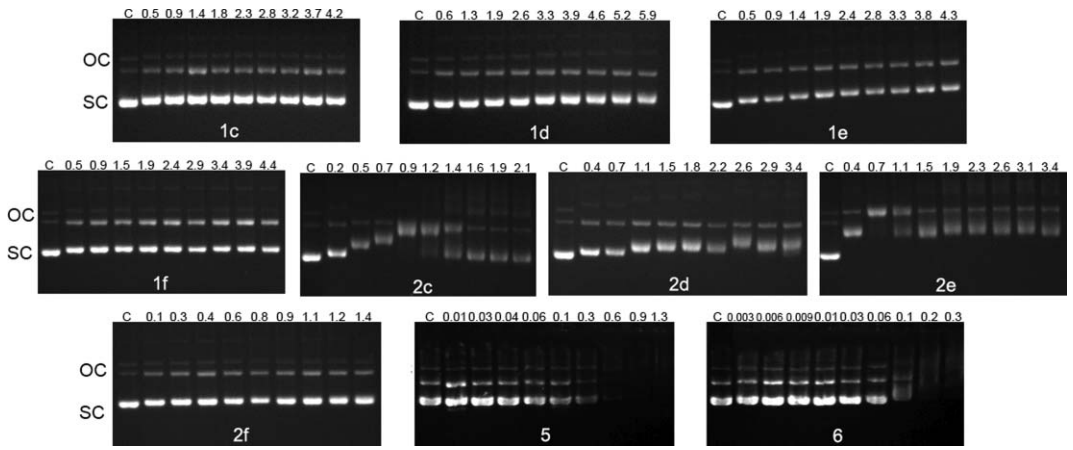

Fig. 2 DNA mobility shift assay for ruthenium complexes **1c–f**, **2c–f**, **5**, and **6**. The range of ruthenium complex concentrations used (mM) is indicated (top of the panels). C is the control lane without the ruthenium complex. OC, open circular plasmidic DNA; SC, supercoiled DNA.

Table 3 Oligonucleotides adducts of the 14-mer 5′-ATACATGGTACATA with different ruthenium complexes observed by MALDI-TOF MS (1 : 5 Oligonucleotide Drug Ratio)

	Complex	Calcd *m*/*z*	Obsd *m*/*z*	Relative abundance (%)	Ruthenium fragment bonded to the oligonucleotide
Entry 1	**2b**	4759.2	4756.4	30%	[Ru{κ^3(*N*,*N*,*N*)-Tp}(1-CH_3-PTA)]
Entry 2		4930.3	4928.8	11%	[Ru{κ^3(*N*,*N*,*N*)-Tp}(1-CH_3-PTA)$_2$]
Entry 3		5021.3	5018.7	10%	[Ru{κ^3(*N*,*N*,*N*)-Tp}(1-CH_3-PTA)(PPh_3)]
Entry 4	**3**	4745.1	4744.5	8%	[Ru{κ^3(*N*,*N*,*N*)-Tp}(PTA)]
Entry 5	**4**	4759.8	4758.7	65%	[Ru{κ^3(*N*,*N*,*N*)-Tp}(1-CH_3-PTA)]
Entry 6		4930.9	4930.8	44%	[Ru{κ^3(*N*,*N*,*N*)-Tp}(1-CH_3-PTA)$_2$]

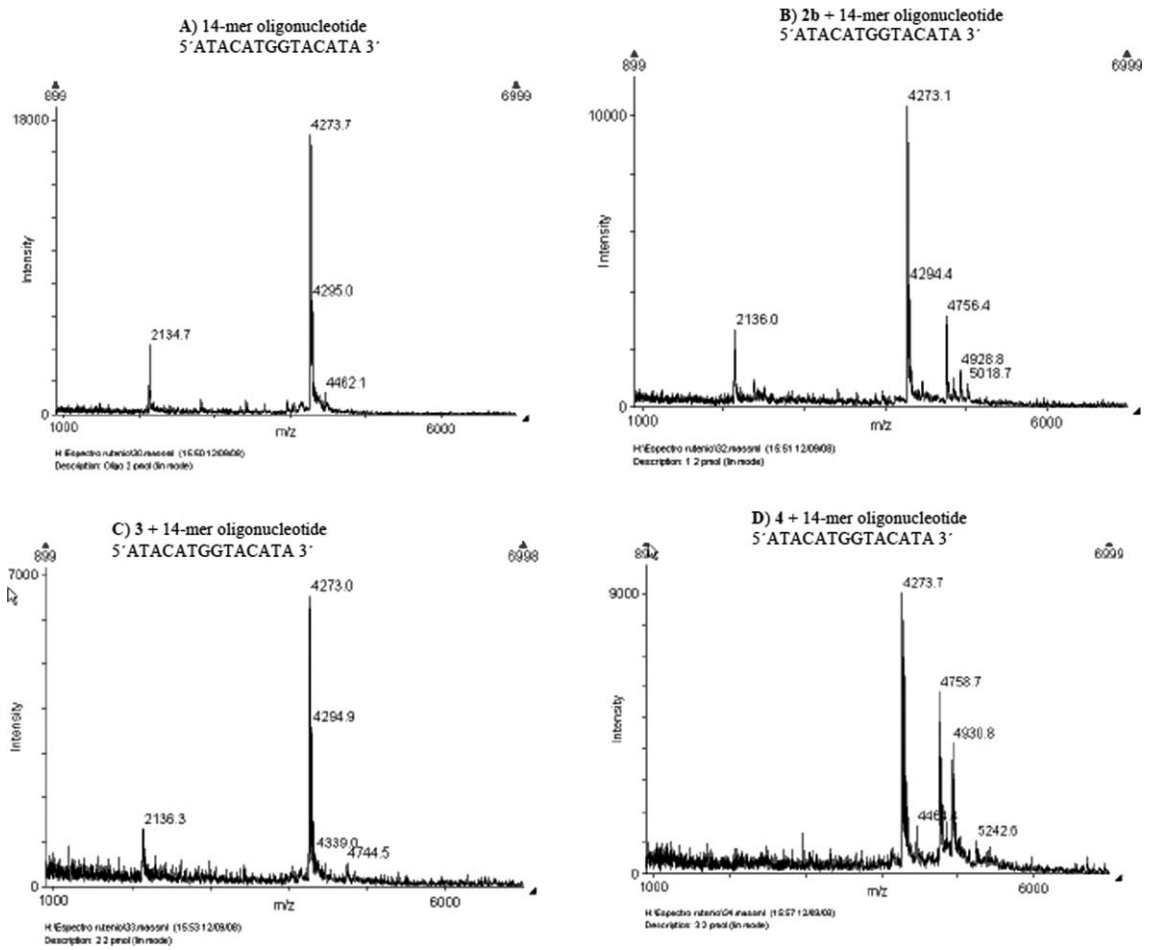

Fig. 3 A) MS spectrum for the oligonucleotide (control, *m*/*z* 4273.7), B–D MS spectra of complexes **2b**, **3**, and **4** incubated with the 14-mer oligonucleotide.

includes the hydrolysis of the chloride ligand and the dissociation of the ancillary phosphane or phosphite ligands. The vacant coordination generated could be occupied by a donor group from the 14-mer oligonucleotide 5′ATACATGGTACATA 3′. Guanine nitrogen-7 has been described as a preferential target for ruthenium(II) complexes,[36–39] even when many ruthenium(II) complexes do not react selectively with nucleobases.

The dissociation of the ancillary ligands, observed for complexes **2b**, **3**, and **4**, seems to indicate that the differences found in the behavior of the complexes with respect to the DNA fragments (see Fig. 2) must be attributed to other factors such as the solubilities or the acid–base properties of the different complexes. Further experiments will be necessary to determine the specific mechanism involved in the interaction between DNA and the ruthenium complexes described here.

In order to determine if the complexes exhibit the same behavior in solution, the stability of these complexes was established in an aqueous solution. Thus, a sample of the complexes was heated at 37° at physiological pH for 14 h. Afterwards, $^{31}P\{^1H\}$NMR experiments indicated no change in the complexes. Furthermore, conductivity experiments discarded hydrolysis of the chloride ion in the complexes.

For the rest of the complexes tested, while bonding to the oligonucleotide was not detected by MALDI-TOF mass spectrometry, their interaction with circular DNA was observed by shift mobility assays in agarose gels (see above and Fig. 2). Consequently, both techniques should be considered complemen-

tary. Thus, a negative result in the MALDI-TOF experiment does not exclude interaction with DNA, while a positive result proves DNA interaction. The differences observed with single or double stranded DNA suggest different interaction mechanisms, which will be interesting to analyze in the future. Mammalian chromosomal DNA is a double helix, however, it becomes single stranded during the replication and transcription processes; so interaction of ruthenium complexes with single strand DNA could also be one of the causes of its antitumor activity.

Biological activity of ruthenium complexes against tumor cell lines. The growth inhibitory activity of compounds **1a–1e**, **2a–2e**, **3–6** was analyzed against well characterized tumor cell lines (NCI-H460, SF-268, MCF-7) (Table 4 and Fig. 4). The complex [$RuCl_2$(*p*-cymene)(PTA)] (RAPTA-C), a well characterized ruthenium complex with antitumor activity,[40–42] and doxorubicin, an antitumor drug used in clinical practice, were used as controls (Table 4 and Fig. 4).

The half maximal inhibitory concentration (IC_{50}) against tumor cell lines of complexes **1a**, **1c**, **2a**, **2c**, **2e**, and [$RuCl_2$(*p*-cymene)(PTA)] (RAPTA-C) was not significant (≥ 10^{-4} M) (Table 4). Compounds **1b** and **1e** are 10 times more effective (IC_{50} in the range of 10^{-5} M). The most active compounds were **2b**, **3**, **4**, **5**, **5′** and **6**, with an IC_{50} against all the analyzed tumor cell lines in the range of low micromolar concentration, only one order of magnitude lower than the antitumor drug doxorubicin widely used in clinical practice.

All of the ruthenium compounds analyzed were less toxic for non-transformed human umbilical vein endothelial cells (HUVEC; normal cells) than doxorubicin (Table 4). Compounds **1b**, **1c**, **1e**, **2a**, **2b**, **2c**, **4**, **5**, and **5′** were the least toxic compounds for HUVEC cells with IC_{50} values of 10^{-5} M, 100-fold lower than doxorubicin. Compounds **1a**, **2e**, **3**, and **6** had IC_{50} values in the range of 10^{-6} which represents 10 times lower toxicity than doxorubicin (Table 4). Compounds **2b**, **3**, **4**, **5** and **5′** were the only ones that showed a therapeutic window (see above), being more efficient against tumor cells than against normal HUVEC cells. Compounds **2b**, **4**, **5** and **5′** achieved the best benefit-to-risk

Table 4 *In vitro* growth inhibitory activity of ruthenium complexes on tumor and normal cells[a]

IC_{50}/μM				
Ru complex	NCI-H460	SF-268	MCF-7	HUVEC
1a	>100	>100	>100	5.0 ± 0.8
1b	27.0 ± 1.4	28.2 ± 2.2	11.3 ± 1.4	25.3 ± 1.1
1c	≥100	29 ± 1.3	≥100	40.1 ± 4.9
1e	32.1 ± 1.3	31.3 ± 1.4	30.3 ± 1.5	93.6 ± 2.2
2a	>100	>100	≥100	58.6 ± 1.4
2b	3.1 ± 0.4	3.4 ± 0.5	4.1 ± 0.5	10.6 ± 0.4
2c	>100	≥100	≥100	9.9 ± 0.7
2e	>100	≥100	≥100	3.6 ± 0.4
3	3.4 ± 0.3	2.6 ± 0.2	3.1 ± 0.3	6.6 ± 0.3
4	3.1 ± 0.3	3.1 ± 0.3	3.3 ± 0.4	27.9 ± 2.7
5	5.1 ± 0.5	4.8 ± 0.5	4.2 ± 0.4	67.0 ± 8.4
5′	4.6 ± 0.4	4.3 ± 0.3	4.7 ± 0.5	24.0 ± 0.5
6	6.1 ± 0.7	2.8 ± 0.1	2.0 ± 0.1	1.9 ± 0.2
Doxorubicin	0.3 ± 0.1	0.3 ± 0.1	0.3 ± 0.1	0.2 ± 0.1
RAPTA-C	>100	>100	>100	>100

[a] Growth inhibitory activity of ruthenium complexes against NCI-H460 lung carcinoma, SF-268 glioblastoma, MCF-7 breast carcinoma, and HUVEC (normal cells) was determined using the XTT assay as described in Materials and methods. Data are shown as the mean values ± S.D. of three experiments performed in triplicate.

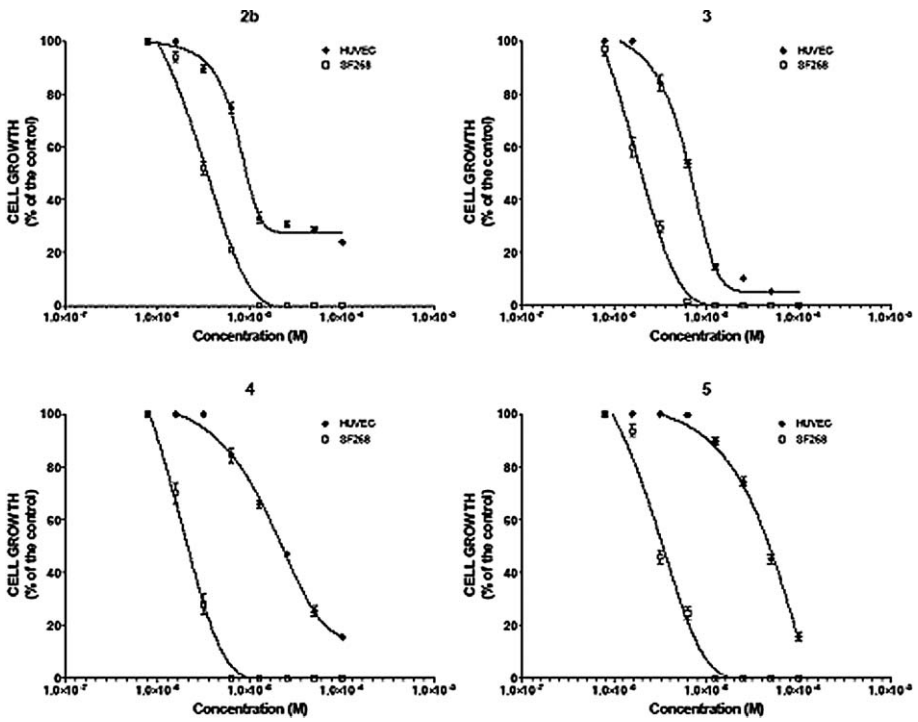

Fig. 4 Effect of compounds **2b**, **3**, **4**, and **5** on cell proliferation of SF-268 glioblastoma cells and HUVEC. Cells were incubated with compounds **2b**, **3**, **4**, and **5** at the indicated concentrations. After 3 days, cell proliferation was determined by the XTT assay and plotted as a percentage of untreated control cells. Results are mean values ± SD of a representative experiment in triplicate, out of three performed.

ratios, with a rather high antitumor activity (IC_{50} values of 10^{-6} M, only 10-fold lower than doxorubicin) and the lowest toxicity against HUVEC non-tumor cells (IC_{50}s of 10^{-5} M, 100-fold lower than doxorubicin) (Table 4 and Fig. 4). Therefore, the compounds **2b**, **4**, **5** and **5′** show a very promising antitumor activity, and further studies and development might be warranted to assess their putative clinical application in cancer chemotherapy. On the other hand, the ability of the drugs to inhibit HUVEC proliferation could suggest an anti-angiogenic effect, as this is a widely used assay to test drugs for their potential anti-angiogenic activity.[43]

As previously discussed, assuming that the ancillary ligands dissociate upon coordination to the ADN, the differences found in the growth inhibitory activity of the different complexes must be attributed to factors other than the ligands (solubilities, electronic properties, *etc.*). On the other hand, the analyses of the behavior of complexes [Ru{κ³(*N*,*N*,*N*)-Tp}(NCMe)(PPh_3)(PTA)][CF_3SO_3] (**5**) and [Ru{κ³(*N*,*N*,*N*)-Tp}(NCMe)(PPh_3)(PTA)][PF_6] (**5′**), indicate that the counteranion effect may not be important for their antitumor activities. Thus, no statistically significant differences ($p > 0.05$, $n = 3$; Student's *t*-test) were observed between the IC_{50} values of complexes **5** and **5′** in all the cells assayed (Table 4).

Interestingly, compounds **2b**, **3**, and **4** were the only compounds that interacted with linear DNA-oligonucleotides, when analyzed by MALDI-MS (see above), and they behaved as very active compounds in inhibiting cancer cell proliferation. This result suggests that the oligonucleotide interaction measured by MALDI-MS might be used to make an initial screening of putative ruthenium complexes with antitumor activity additional to plasmid mobility shift assay. However, it is evident that, in order to characterize the activity and to determine the specific cellular targets of these novel compounds, more detailed analysis of their interactions with DNA and other cellular molecules will be necessary, by a range of additional chemical–biochemical techniques. These experiments will provide a valuable information of their properties prior to the *in vitro* cellular cultures analyses and *in vivo* tests with animals.

Experimental

All manipulations were performed in an atmosphere of dry nitrogen using vacuum-line and standard Schlenk techniques. All reagents were obtained from commercial suppliers and used without further purification. Solvents were dried by standard methods and distilled under nitrogen before use. The compounds [RuCl{κ³(*N*,*N*,*N*)-Tp}($PTA)_2$] (**1a**), [RuCl{κ³(*N*,*N*,*N*)-Tp}(1-CH_3-$PTA)_2$][CF_3SO_3]$_2$ (**2a**), [RuCl{κ³(*N*,*N*,*N*)-Tp}(PPh_3)(PTA)] (**1b**), [RuCl{κ³(*N*,*N*,*N*)-Tp}(PPh_3)(1-CH_3-PTA)][CF_3SO_3] (**2b**), [RuH{κ³(*N*,*N*,*N*)-Tp}(PPh_3)(PTA)] (**3**), [RuH{κ³(*N*,*N*,*N*)-Tp}(PPh_3)(1-CH_3-PTA)][CF_3SO_3] (**4**), and [Ru{κ³(*N*,*N*,*N*)-Tp}(NCMe)(PPh_3)(PTA)][PF_6] (**5**) were prepared following previously reported methods.[14] Infrared spectra were recorded on a Perkin-Elmer FT-IR Paragon 1000 spectrometer. The C, H, and N analyses were carried out with a Perkin-Elmer 240-B microanalyzer. Cyclic voltammetry measurements (25 °C) were carried out with a three-electrode system, using a platinum disk, a platinum wire and a silver wire as working, counter and reference electrodes respectively. Current and voltage parameters were controlled by using a μ-AUTOLAB Type III. In a typical experiment, complex was dissolved under a nitrogen atmosphere in recently distilled and deoxygenated DMF in the complexes and 0.15 M in [Bu_4N][BF_4] as electroyte. The potentials of the complexes were measured by CV in the presence of the couple [Fe(η-$C_5H_5)_2$]$^{0/+}$ as the internal standard. NMR spectra were recorded on Bruker AC-400 instruments at 400.1 MHz (^{1}H), 161.9 (^{31}P), or 100.6 MHz (^{13}C) using $SiMe_4$ or 85% H_3PO_4 as standards. DEPT experiments were carried out for all the compounds. Coupling constants *J* are expressed in Hertz. Resonances due to the Tp ligand are reported by chemical shift and multiplicity, since all $^3J_{HH}$ values for pyrazolyl rings are 2 Hz. Abbreviations used: br, broad signal; s, singlet; d, doublet; m, multiplet; q, quartet; quin, quintuplet; sext, sextuplet; t, triplet. Full characterization for one characteristic complex of each family is provided. For the rest of the complexes, full characterization can be found in the ESI.†

Oligonucleotide binding. MALDI mass spectrometry

The 14-mer oligonucleotide 5′ATACATGGTACATA 3′was obtained from Sigma-Aldrich. Samples were prepared to a final concentration of oligonucleotide of 2 pmol/μl in ammonium phosphate buffer at physiological pH 7.0. Ruthenium complexes were added to achieve a stoichiometric ratio of 1 : 5 (10 pmol/μl of Ru complex). Reaction mixtures were incubated for 14 h at 37 °C. Two pmols (1 μl) were processed for MALDI mass spectrometry. A Perseptive Voyager STR instrument with 3-hydroxypicolinic acid matrix was used, detecting positive ions in a reflector TOF mass analyzer in linear mode.

DNA mobility shift assays

Reactions between DNA and the ruthenium complexes were performed in 10 mM sodium phosphate buffer at physiological pH 7.0, containing 0.05 μg μL^{-1} of the pBR322 plasmid (4361 base pairs, from Fermentas) and appropriate amounts of freshly prepared solutions of the Ru complexes, also dissolved in phosphate buffer. For each compound different dilutions were used as a function of their maximum solubility. Reaction mixtures were incubated for 14 h at 37 °C. Ten microlitres of the reactions were mixed with 1 μL dye (0.025 mg bromophenol blue, 1mL glycerol, and 1 mL distilled water) and analyzed by electrophoresis in 0.8% agarose gels in TBE (Tris-Borate-EDTA) buffer. Gel running was conducted at a constant voltage of 3 V cm^{-1}. DNA bands were visualized by incubating the gel with 1 μg mL^{-1} ethidium bromide in TBE buffer for 10 min, after which time they were photographed under UV light.

Cell culture

NCI-H460 (human large cell carcinoma of the lung), SF-268 (human glioblastoma), and MCF-7 (human breast adenocarcinoma) cells were cultured in DMEM culture medium containing 10% (v/v) heat-inactivated fetal bovine serum (FBS), 2 mM L-glutamine, 100 U/ml penicillin, and 100 μg ml^{-1} streptomycin at 37 °C in air containing 95% humidity and 5% CO_2. Cells were periodically tested for *Mycoplasma* infection using the MycoAlert© Mycoplasma detection kit (Lonza, Basel, Switzerland) as well as the Venor©GeM Advance Mycoplasma PCR detection Kit (Minerva Biolabs, Berlin, Germany), and found to be negative.

Human umbilical vein endothelial cells (HUVEC) were obtained by collagenase digestion of umbilical cord veins as previously described.[44]

Cell growth inhibition assay

The effect of the distinct compounds in the proliferation of human tumor cell lines (cytostatic activity) was determined as previously described[45] by using the XTT (sodium 3′-[1-(phenylaminocarbonyl)-3,4-tetrazolium]-bis (4-methoxy-6-nitro) benzene sulfonic acid hydrate) cell proliferation kit (Roche Molecular Biochemicals, Mannheim, Germany) according to the manufacturer's instructions. Cells (1.5×10^3 in 100 µl) were incubated in DMEM culture medium containing 10% heat-inactivated FBS, in the absence and in the presence of the indicated compounds at a concentration range of 10^{-4} to 10^{-9} M, in 96-well flat-bottomed microtiter plates, and following 72 h of incubation at 37 °C in a humidified atmosphere of air/CO_2 (19/1) the XTT assay was performed. Measurements were done in triplicate, and each experiment was repeated three times. The IC_{50} (50% inhibitory concentration) value, defined as the drug concentration required to cause 50% inhibition in the cellular proliferation with respect to the untreated controls, was determined for each compound. Non-linear curves fitting the experimental data were carried for each compound.

Synthesis of complexes [RuCl{κ³(*N*,*N*,*N*)-Tp}(L)(PTA)] (L = PMe_2Ph (1c), PMe_3 (1d), $P(OMe)_3$ (1e), $P(OPh)_3$ (1f)). To a solution of [RuCl{κ³(*N*,*N*,*N*)-Tp}(PPh_3)(PTA)] complex (100 mg, 0.13 mmol) in toluene (10 mL), an excess of the corresponding phosphane or phosphite was added and the mixture was heated at reflux temperature. Once the reaction was completed, the solvent was removed under reduced pressure and the solid residue was dissolved in dichloromethane (0.5 mL). Addition of hexane (60 mL) afforded the desired product as a pale yellow (**1c**) or white (**1d–f**) precipitate. In the synthesis of [RuCl{κ³(*N*,*N*,*N*)-Tp}(PMe_3)(PTA)] complex (**1d**), the reaction mixture was heated at 125 °C using a pressure tube. **1c** (56 mg, 67%): Stoichiometry 1 : 1.5. Reaction time: 6 h. $S_{20\,°C}$ (H_2O) = 3.0 mg mL^{-1}. IR(KBr): ν_{max}/cm^{-1} 2462 (BH). ^{1}H-NMR δ_H(400.1 MHz, CD_2Cl_2, 20 °C) 8.02 (d, 1H, $H^{3,5}$ (pz)), 7.80 (d, 1H, $H^{3,5}$ (pz)), 7.69 (d, 1H, $H^{3,5}$ (pz)), 7.65 (d, 1H, $H^{3,5}$ (pz)), 7.58 (d, 1H, $H^{3,5}$ (pz)), 7.45–7.35 (m, 5H, Ph), 7.13 (d, 1H, $H^{3,5}$ (pz)), 6.25 (t, 1H, H^4 (pz)), 6.19 (t, 1H, H^4 (pz)), 6.05 (t, 1H, H^4 (pz)), 4.44 (AB spin system, 3H, J_{AB} = 13 Hz, NCH_2N), 4.28 (AB spin system, 3H, J_{AB} = 13 Hz, NCH_2N), 3.95 (AB spin system, 3H, J_{AB} = 15 Hz, NCH_2P), 3.71 (AB spin system, 3H, J_{AB} = 15 Hz, NCH_2P), 1.89 (d, 3H, $^2J_{HP}$ = 9 Hz, $P(CH_3)_2Ph$), 1.55 (d, 3H, $^2J_{HP}$ = 9 Hz, $P(CH_3)_2Ph$). ^{13}C- NMR δ_C(100.6 MHz, CD_2Cl_2, 20 °C) 147.1 (C-3 (pz)), 143.5 (C-3(pz)), 143.0 (C-3 (pz)), 142.3 (d, J_{CP} = 37 Hz, C-1 Ph), 136.3 (C-5 (pz)), 135.5 (C-5 (pz)), 129.9 (d, 2C, $^2J_{CP}$ = 8 Hz, C-2,6 Ph), 128.9 (C-4 Ph), 128.4 (d, 2C, $^3J_{CP}$ = 8 Hz, C-3,5 Ph), 105.7 (C-4 (pz)), 105.1 (C-4 (pz)), 104.9 (C-4 (pz)), 73.2 (d, 3C, $^3J_{CP}$ = 5 Hz, NCH_2N), 52.2 (d, 3C, J_{CP} = 14 Hz, NCH_2P), 17.1 (d, J_{CP} = 29 Hz, $P(CH_3)_2Ph$), 15.2 (d, J_{CP} = 29 Hz, $P(CH_3)_2Ph$). ^{31}P-NMR δ_P(161.9 MHz, CD_2Cl_2, 20 °C) 21.1 (d, $^2J_{PP}$ = 36 Hz, PMe_2Ph), −26.6 (d, $^2J_{PP}$ = 36 Hz, PTA). Found: C, 42.68; H, 4.75; N,19.52. Calc. for $C_{23}H_{33}BClN_9P_2Ru$: C, 42.84; H, 5.16; N, 19.55.

Synthesis of complexes [RuCl{κ³(*N*,*N*,*N*)-Tp}(L)(1-CH_3-PTA)][CF_3SO_3] (L = PMe_2Ph (2c), PMe_3 (2d), $P(OMe)_3$ (2e), $P(OPh)_3$ (2f)). Methyl triflate (16 µL, 0.13 mmol) was added to a solution of the corresponding complex [RuCl{k³(*N*,*N*,*N*)-Tp}(L)(PTA)] (L = PMe_2Ph (**1c**), PMe_3 (**1d**), $P(OMe)_3$ (**1e**), $P(OPh)_3$ (**1f**)) (0.13 mmol) in dichloromethane (2 mL) at −30 °C. The reaction mixture was stirred at −30 °C for 40 min. Addition of hexane (30 mL) afforded a precipitate. The solvents were decanted and the solid was washed with hexane (3 × 5 mL) and dried under reduced pressure. **2c** (66 mg, 63%): Conductivity (acetonitrile, 20 °C): Λ = 128 S cm^2 mol^{-1}. $S_{20\,°C}$ (H_2O) = 1.9 mg mL^{-1}. IR (KBr): ν_{max}/cm^{-1} 2481 (BH), 1258, 1163, 1031 (CF_3SO_3). ^{1}H-NMR δ_H(400.1 MHz, acetonitrile-d_3, 20 °C) 8.04 (d, 1H, $H^{3,5}$ (pz)), 7.90 (d, 1H, $H^{3,5}$ (pz)), 7.78 (d, 1H, $H^{3,5}$ (pz)), 7.72 (d, 1H, $H^{3,5}$ (pz)), 7.56 (d, 1H, $H^{3,5}$ (pz)), 7.43–7.34 (m, 6H, Ph and $H^{3,5}$ (pz)), 6.29 (br, 2H, H^4 (pz)), 6.06 (t, 1H, H^4 (pz)), 4.75–4.65 (m, 4H, 1-CH_3-PTA), 4.31–3.65 (m, 6H, 1-CH_3-PTA), 3.55 (AB spin system, 1H, J_{AB} = 15 Hz, 1-CH_3-PTA), 3.34 (AB spin system, 1H, J_{AB} = 15 Hz, 1-CH_3-PTA), 2.62 (s, 3H, CH_3N), 1.83 (d, 3H, $^2J_{HP}$ = 9 H, $P(CH_3)_2Ph$), 1.49 (d, 3H, $^2J_{HP}$ = 9 Hz, $P(CH_3)_2Ph$). ^{13}C- NMR δ_C(100.6 MHz, acetonitrile-d_3, 20 °C) 147.9 (C-3 (pz)), 143.9 (C-3 (pz)), 143.2 (C-3 (pz)), 141.7 (d, J_{CP} = 43 Hz, C-1 Ph), 136.9 (C-5 (pz)), 135.7 (C-5 (pz)), 135.4 (C-5 (pz)), 129.9 (d, 2C, $^2J_{CP}$ = 9 Hz, C-2,6 Ph), 129.4 (C-4 Ph), 128.8 (d, 2C, $^2J_{CP}$ = 9 Hz, C-3,5 Ph), 121.2 (q, J_{CF} = 254 Hz, CF_3SO_3), 106.7 (C-4 (pz)), 105.7 (C-4 (pz)), 105.2 (C-4 (pz)), 80.4 (d, 2C, $^3J_{CP}$ = 3 Hz, CH_3NCH_2N), 69.0 (d, $^3J_{CP}$ = 5 Hz, NCH_2N), 57.7 (d, J_{CP} = 6 Hz, CH_3NCH_2P), 49.0 (CH_3N), 48.3 (d, J_{CP} = 15 Hz, NCH_2P), 47.9 (d, J_{CP} = 15 Hz, NCH_2P), 16.3 (d, J_{CP} = 30 Hz, $P(CH_3)_2Ph$), 14.2 (d, J_{CP} = 30 Hz, $P(CH_3)_2Ph$). ^{31}P-NMR δ_P(161.9 MHz, acetonitrile-d_3, 20 °C) 18.8 (d, J_{PP} = 35 Hz, PMe_2Ph), −8.2 (d, J_{PP} = 35 Hz, 1-CH_3-PTA). Found: C, 36.30; H, 5.52; N, 15.08; S, 3.86 (M^+, 660). Calc. for $C_{25}H_{36}BClF_3N_9O_3P_2RuS \cdot 1/4CH_2Cl_2$: C, 36.53; H, 5.43; N, 15.18; S, 3.86.

Synthesis of complex [Ru{κ³(*N*,*N*,*N*)-Tp}(NCMe)(PPh_3)-(PTA)][CF_3SO_3] (5). Sodium triflate (0.39 mmol) was added to a solution of complex [RuCl{k³(*N*,*N*,*N*)-Tp}(PPh_3)(PTA)] (100 mg, 0.13 mmol) in an acetonitrile–methanol mixture (12 mL, 1 : 5). The reaction mixture was heated at reflux temperature for 5 h. The solution was cooled to room temperature and the solvents were removed under reduced pressure. The solid residue obtained was extracted with dichloromethane and the resulting solution filtered through Kieselguhr. The solution was then concentrated under reduced pressure to *ca.* 1 mL. Addition of diethyl ether afforded a white precipitate. The solvents were decanted and the solid residue was washed with diethyl ether (2 × 5 mL) and dried under reduced pressure. **5** (54 mg, 45%): Conductivity (acetonitrile, 20 °C): Λ = 102 S cm^2 mol^{-1}. $S_{20\,°C}$ (H_2O) = 1.3 mg mL^{-1}. IR (KBr): ν_{max}/cm^{-1} 2488 (BH)), 1264, 1159, 1030 (CF_3SO_3). ^{1}H-NMR δ_H(400.1 MHz, CD_2Cl_2, 20 °C) 8.12 (d, 1H, $H^{3,5}$ (pz)), 8.02 (d, 1H, $H^{3,5}$ (pz)), 7.87 (d, 1H, $H^{3,5}$ (pz)), 7.81 (d, 1H, $H^{3,5}$ (pz)), 7.49–7.47 (m, 3H, PPh_3), 7.43–7.41 (m, 6H, PPh_3), 7.39 (d, 1H, $H^{3,5}$ (pz)), 7.22–7.17 (m, 6H, PPh_3), 6.65 (d, 1H, $H^{3,5}$ (pz)), 6.38 (t, 1H, H^4 (pz)), 6.27 (t, 1H, H^4 (pz)), 6.02 (t, 1H, H^4 (pz)), 4.41 (AB spin system, 3H, J_{HAHB} = 13 Hz, NCH_2N), 4.32 (AB spin system, 3H, J_{HAHB} = 13 Hz, NCH_2N), 3.98 (CD spin system, 3H, J_{HCHD} = 15 Hz, NCH_2P), 3.64 (CD spin system, 3H, J_{HCHD} = 15 Hz, NCH_2P), 2.27 (s, 3H, $NCCH_3$). ^{13}C- NMR δ_C(100.6 MHz, CD_2Cl_2, 20 °C)

147.1 (C-3 (pz)), 144.3 (C-3 (pz)), 142.5 (C-3 (pz)), 137.8 (C-5 (pz)), 136.4 (C-5 (pz)), 136.2 (C-5 (pz)), 134.2 (d, 6C, $^{2}J_{CP}$ = 9 Hz, C-2,6 PPh_3), 134.0 (d, 3C, J_{CP} = 29 Hz, C-1 PPh_3), 130.4 (3C, C-4 PPh_3), 128.5 (d, 6C, $^{3}J_{CP}$ = 8 Hz, C-3,5 PPh_3), 126.0 (N*C*CH_3), 121.1 (q, J_{CF} = 321 Hz, *C*F_3SO_3), 107.0 (3C, C-4 (pz)), 106.6 (C-4 (pz)), 106.4 (C-4 (pz)), 72.7 (d, 3C, $^{3}J_{CP}$ = 5 Hz, N*C*H_2N), 50.8 (d, 3C, J_{CP} = 13 Hz, N*C*H_2P), 4.41 (NC*C*H_3). ^{31}P-NMR δ_P(161.9 MHz, CD_2Cl_2, 20 °C) 44.2 (d, J_{PP} = 29 Hz, PPh_3), –42.5 (d, J_{PP} = 29 Hz, PTA). Found: C, 46.34; H, 4.32; N, 15.08; S, 3.32. Calc. for $C_{36}H_{40}BF_3N_{10}O_3P_2RuS$: C,46.81; H, 4.36; N, 15.16; S, 3.47.

Synthesis of complex [Ru{κ³(*N*,*N*,*N*)-Tp}(NCMe)(PPh_3)(1-CH_3-PTA)][CF_3SO_3]$_2$ (6). Methyl triflate (16 μL, 0.13 mmol) was added to a solution of complex [Ru{k³(*N*,*N*,*N*)-Tp}(NCMe)(PPh_3)(PTA)][CF_3SO_3] (**5**) (120 mg, 0.13 mmol) in dichloromethane (2 mL) at –30 °C. The reaction mixture was stirred at –30 °C for 40 min. Addition of hexane (30 mL) afforded a precipitate. The solvents were decanted and the solid obtained was washed with hexane (3 × 5 mL) and dried under reduced pressure. **6** (37 mg, 68%): Conductivity (acetonitrile, 20 °C): Λ = 233 S cm^2 mol^{-1}. $S_{20\,°C}$ (H_2O) = 0.33 mg mL^{-1}. IR (KBr): ν_{max}/cm^{-1} 2492 (BH), 1257, 1163, 1031 (CF_3SO_3). ^{1}H-NMR δ_H(400.1 MHz, acetonitrile-d_3, 20 °C) 8.13 (d, 1H, H^{3,5} (pz)), 8.11 (d, 1H, H^{3,5} (pz)), 7.96 (d, 1H, H^{3,5} (pz)), 7.92 (d, 1H, H^{3,5} (pz)), 7.55–7.51 (m, 4H, PPh_3 and H^{3,5} (pz)), 7.46–7.42 (m, 6H, PPh_3), 7.19–7.15 (m, 6 H, PPh_3), 6.66 (d, 1H, H^{3,5} (pz)), 6.41 (t, 1H, H^4 (pz)), 6.33 (t, 1H, H^4 (pz)), 6.05 (t, 1H, H^4 (pz)), 4.84–4.75 (m, 4H, CH_3NCH_2N), 4.33–4.16 (m, 3H, NCH_2N, and CH_3NCH_2P), 3.84–3.78 (m, 2H, CH_3NCH_2P and NCH_2P), 3.72–3.71 (m, 1H, NCH_2P), 3.50–3.48 (m, 1H, NCH_2P), 3.45–3.35 (m, 1H, NCH_2P), 2.68 (s, 3H, CH_3NCH_2N), 2.25 (s, 3H, NCCH_3). ^{13}C- NMR δ_C (100.6 MHz, acetonitrile-d_3, 20 °C) 148.4 (C-3 (pz)), 144.5 (C-3 (pz)), 143.0 (C-3 (pz)), 138.4 (C-5 (pz)), 137.2 (C-5 (pz)), 137.1 (C-5 (pz)), 134.3 (d, $^{2}J_{CP}$ = 9 Hz, C-2,6 PPh_3), 133.3 (d, J_{CP} = 42 Hz, C-1 PPh_3), 130.8 (C-4 PPh_3), 128.7 (d, $^{3}J_{CP}$ = 9 Hz, C-3,5 PPh_3), 127.5 (N*C*CH_3), 121.0 (q, J_{CF} = 320 Hz, *C*F_3SO_3), 107.8 (C-4 (pz)), 107.2 (C-4 (pz)), 106.7 (C-4 (pz)), 80.3 (CH_3N*C*H_2N), 80.2 (CH_3N*C*H_2N), 68.7 (d, $^{3}J_{CP}$ = 5 Hz, N*C*H_2N), 55.9 (d, J_{CP} = 8 Hz, CH_3N*C*H_2P), 49.1 (*C*H_3NCH_2N), 46.7 (d, J_{CP} = 15 Hz, N*C*H_2P), 46.5 (d, J_{CP} = 16 Hz, N*C*H_2P), 4.1 (NC*C*H_3). ^{31}P-NMR δ_P (161.9 MHz, acetonitrile-d_3, 20 °C) 39.7 (d, J_{PP} = 28 Hz, PPh_3), –16.7 (d, J_{PP} = 28 Hz, 1-CH_3-PTA). Found: C, 42.27; H, 4.03; N, 13.11; S, 6.21. Calc. for $C_{38}H_{43}BF_6N_{10}O_6P_2RuS_2$: C, 41.96; H, 3.98; N, 12.88; S, 5.90.

X-ray crystal structure determination of complex 2c·2NCMe. Crystals suitable for X-ray diffraction analysis were obtained by slow evaporation of a saturated solution of complex **2c** in acetonitrile. The most relevant crystal and refinement data are reflected in Table 5.

Diffraction data were recorded at 150(2) K on a Nonius KappaCCD single crystal diffractometer using Mo-Kα radiation, λ = 0.71073 Å. Crystal–detector distance was fixed at 35 mm and the oscillation method was used, with 1° oscillation and 30 s exposure time per frame. The data collection strategy was calculated by the program Collect.[46] Data reduction and cell refinement were performed using the programs HKL Denzo and Scalepack[47] and absorption correction was performed by means of Sortav.[48]

Table 5 Crystal data and structure refinement for complex [RuX{κ³(*N*,*N*,*N*)-Tp}(PMe_2Ph)(1-CH_3-PTA)]·2NCMe (**2c**·2NCMe)

	2c·2NCMe
Empirical formula	$C_{24}H_{36}BClN_9P_2Ru$, CF_3SO_3, 2(CH_3CN)
fw	891.07
T/K	150(2)
Wavelength/Å	0.71073
Crystal system	Triclinic
Space group	$P\bar{1}$
a/Å	11.8579(10)
b/Å	13.2648(1)
c/Å	14.3777(1)
α (°)	62.978(4)
β (°)	76.385(3)
γ (°)	76.013(4)
Z	2
Volume/Å^3	1934.15 (16)
$\rho_{calculated}$/g cm^{-3}	1.530
μ/mm^{-1}	0.673
F(000)	912
Crystal size/mm	0.27 × 0.25 × 0.20
θ range (deg)	1.61 to 25.24
No. reflns. collected	30790
No. unique reflns.	6808 [*R*(int) = 0.0258]
Completeness to θ_{max}	97.2%
No. parameters/restraints	593/0
Goodness-of-fit on F^2	1.209
R_1 [$I > 2\sigma(I)$][a]	0.0354
wR_2 [$I > 2\sigma(I)$][b]	0.1000
R_1 (all data)	0.0424
wR_2 (all data)	0.1237
Largest diff. peak and hole/e Å^{-3}	1.109 and –1.140

[a] $R_1 = \Sigma(|F_o| - |F_c|)/\Sigma|F_o|$; [b] $wR_2 = \{\Sigma[w(F_o^2 - F_c^2)^2]/\Sigma[w(F_o^2)^2]\}^{\frac{1}{2}}$.

The software package WINGX was used for space group determination, structure solution, and refinement.[49] The structures were solved by Patterson interpretation and phase expansion using DIRDIF.[50] In the crystal, two acetonitrile molecules of solvation per one formula unit of the complex were found. Anisotropic least-squares refinement was carried out with SHELXL-97.[51] During the final stages of refinement, all positional parameters and anisotropic temperature factors of all the non-H atoms were refined. The coordinates of the H atoms were found from difference Fourier maps and included in the refinement with isotropic parameters (except the H atoms of methyl groups, (for C_8, C_9, C_{28}, C_{29}) which were geometrically placed riding on their parent atoms with isotropic displacement parameters set to 1.5 times the U_{eq} of the atoms to which they are attached).

The minimized function was $[\Sigma wF_o^2 - F_c^2)/\Sigma w(F_o^2)]^{1/2}$ where $w = 1/[\sigma^2(F_o^2) + (0.764P)^2 + 1.1361P]$ with $\sigma^2(F_o^2)$ from counting statistics and $P = (\text{Max}\,(F_o^2 + 2F_c^2)/3$.

Atomic scattering factors were taken from the International Tables for X-ray Crystallography.[52] Geometrical calculations were made with PARST.[53] The crystallographic plots were made using PLATON.[54]

Conclusion

A new series of hydridotris(pyrazolyl)borate ruthenium(II) complexes containing the water-soluble phosphanes PTA and 1-CH_3-PTA have been described. Ancillary ligands with different

electronic or steric properties have been included in order to study their influence on the biological activity of the complexes. MALDI experiments confirm the coordination of the fragments [Ru{κ³(*N*,*N*,*N*)-Tp}(PTA)] or [Ru{κ³(*N*,*N*,*N*)-Tp}(1-CH_3-PTA)] to a single strand DNA chain. Most of the new complexes described in this work interact with DNA, and have an inhibitory effect against human tumor cell lines. Remarkably, compounds **2b**, **3**, **4**, **5** and **5′** have an antitumor activity (IC_{50}, 10^{-6} M) that is much stronger than those reported for other ruthenium complexes and is close to the antitumor activity of anticancer drugs currently used in clinical practice, such as doxorubucin. Furthermore, the effect shown on HUVEC cells suggests that the ruthenium(II) complexes analyzed might act as potential anti-angiogenic agents. Further work will be necessary to establish the possible clinical application of these interesting compounds.

Acknowledgements

This work was supported by the Spanish Ministry of Science and Innovation (CTQ2006-08485, SAF2008-02251), Consolider Ingenio 2010 (CSD2007-00006), and Red Temática de Investigación Cooperativa en Cáncer, Instituto de Salud Carlos III, cofunded by the Fondo Europeo de Desarrollo Regional of the European Union (RD06/0020/1037). A. García-Fernández thanks the Spanish Ministry of Education and Science for a scholarship. We also thank Anette Rasmussen, Department of Biochemistry and Molecular Biology, University of Southern Denmark, for her assistance with the MALDI-TOF MS experiments.

Notes and references

1 P. C. A. Bruijnincx and P. J. Sadler, *Adv. Inorg. Chem.*, 2009, **61**, 1–62.
2 P. J. Dyson and G. Sava, *Dalton Trans.*, 2006, 1929–1933.
3 C. S. Allardyce, A. Dorcier, C. Scolaro and P. J. Dyson, *Appl. Organomet. Chem.*, 2005, **19**, 1–10.
4 A. Bergamo, A. Masi, P. J. Dyson and G. Sava, *Int. J. Oncol.*, 2008, **33(6)**, 1281–1289.
5 A. Casini, C. Gabbiani, F. Sorrentino, M. P. Rigobello, A. Bindoli, T. J. Geldbach, A. Marrone, N. Re, C. G. Hartinger, P. J. Dyson and L. Messori, *J. Med. Chem.*, 2008, **51**, 6773–6781.
6 T. Bugarcic, O. Novakova, A. Halamikova, L. Zerzankova, O. Vrana, J. Kasparkova, A. Habtemariam, S. Parsons, P. J. Sadler and V. Brabec, *J. Med. Chem.*, 2008, **51**, 5310–5319.
7 P. C. A. Bruijnincx and P. J. Sadler, *Curr. Opin. Chem. Biol.*, 2008, **12**, 197–206.
8 M. A. Jakupec, M. Galanski, V. B. Arion, C. G. Hartinger and B. K. Keppler, *Dalton Trans.*, 2008, 183–194.
9 J. M. Rademake-Lakhai, D. van den Bongard, D. Pluim, J. H. Beijnen and J. H. M. Schellens, *Clin. Cancer Res.*, 2004, **10**, 3717–3727.
10 C. G. Hartinger, S. Zorbas-Seifried, M. A. Jakupec, B. Kynast, H. Zorbas and B. K. Keppler, *J. Inorg. Biochem.*, 2006, **100**, 891–904.
11 I. Bratsos, S. Jedner, T. Gianferrara and E. Alessio, *Chimia*, 2007, **61**, 692–697.
12 S. J. Dougan and P. J. Sadler, *Chimia*, 2007, **61**, 704–715.
13 W. Kandioller, C. G. Hartinger, A. A. Nazarov, J. Kasser, R. John, M. A. Jakupec, V. B. Arion, P. J. Dyson and B. K. Keppler, *J. Organomet. Chem.*, 2009, **694**, 922–929.
14 T. Bugarcic, A. Habtemariam, J. Stepankova, P. Heringova, J. Kasparkova, R. J. Deeth, R. D. L. Johnstone, A. Prescimone, A. Parkin, S. Parsons, V. Brabec and P. J. Sadler, *Inorg. Chem.*, 2008, **47**, 11470–11486.
15 Y. K. Yan, M. Melchart, A. Habtemariam and P. J. Sadler, *Chem. Commun.*, 2005, 4764–4776.
16 A. D. Phillips, L. Gonsalvi, A. Romerosa, F. Vizza and M. Peruzzini, *Coord. Chem. Rev.*, 2004, **248**, 955–993.
17 A. Renfrew, *Chimia*, 2009, **63**, 217–219.
18 C. A. Vock, A. K. Renfrew, R. Scopelliti, L. Juillerat-Jeanneret and P. J. Dyson, *Eur. J. Inorg. Chem.*, 2008, 1661–1671.
19 C. Scolaro, C. G. Hartinger, C. S. Allardyce, B. K. Keppler and P. J. Dyson, *J. Inorg. Biochem.*, 2008, **102**, 1743–1748.
20 W. H. Ang and P. J. Dyson, *Eur. J. Inorg. Chem.*, 2006, 4003–4018.
21 A. Habtemariam, M. Melchart, R. Fernández, S. Parsons, I. D. H. Oswald, A. Parkin, F. P. A. Fabbiani, J. E. Davidson, A. Dawson, R. E. Aird, D. I. Jodrell and P. J. Sadler, *J. Med. Chem.*, 2006, **49**, 6858–6868.
22 A. K. Renfrew, A. D. Phillips, A. E. Egger, C. G. Hartinger, S. S. Bosquain, A. A. Nazarov, B. K. Keppler, L. Gonsalvi, M. Peruzzini and P. J. Dyson, *Organometallics*, 2009, **28**, 1165–1172.
23 M. H. Garcia, T. S. Morais, P. Florindo, M. F. M. Piedade, V. Moreno, C. Ciudad and V. Noe, *J. Inorg. Biochem.*, 2009, **103**, 354–361.
24 A. Romerosa, M. Saoud, T. Campos-Malpartida, C. Lidrissi, M. Serrano-Ruiz, M. Peruzzini, J. A. Garrido-Cárdenas and F. García-Maroto, *Eur. J. Inorg. Chem.*, 2007, 2803–2812.
25 A. Romerosa, T. Campos-Malpartida, C. Lidrissi, M. Saoud, M. Serrano-Ruiz, M. Peruzzini, J. A. Garrido-Cárdenas and F. García-Maroto, *Inorg. Chem.*, 2006, **45**, 1289–1298.
26 S. Trofimenko, *Chem. Rev.*, 1993, **93**, 943–980.
27 C. Slugovc, R. Schmid and K. Kirchner, *Coord. Chem. Rev.*, 1999, **185–186**, 109–126.
28 A. García-Fernandez, J. Díez, A. Manteca, J. Sánchez, M. P. Gamasa and E. Lastra, *Polyhedron*, 2008, **27**, 1214–1228.
29 A. García-Fernández, J. Díez, M. P. Gamasa and E. Lastra, *Inorg. Chem.*, 2009, **48**, 2471–2481.
30 B. Buriez, I. D. Burns, A. F. Hill, A. J. P. White, D. J. Williams and J. D. E. T. Wilton-Ely, *Organometallics*, 1999, **18**, 1504–1516.
31 S. Pavlik, K. Mereiter, M. Puchberger and K. Kirchner, *J. Organomet. Chem.*, 2005, **690**, 5497–5507and references therein.
32 M. Jiménez-Tenorio, M. D. Palacios, M. C. Puerta and P. Valerga, *Organometallics*, 2005, **24**, 3088–3098and references therein.
33 T. G. Appleton, H. C. Clark and L. E. Manzer, *Coord. Chem. Rev.*, 1973, **10**, 335–422.
34 Analogous reversible behavior has been observed for complexes [RuCl{κ³(*N*,*N*,N)-Tp}(L)(1-BH_3-PTA)]S. Bolaño, J. Bravo, J. Castro, M. M. Rodríguez-Rocha, M. F. C. Guedes da Silva, A. J. L. Pombeiro, L. Gonsalvi and M. Peruzzini, *Eur. J. Inorg. Chem.*, 2007, 5523–5532.
35 For compounds **2b** and **4**, coordination of the fragment [Ru{κ³(*N*,*N*,*N*)-Tp}(1-CH_3-PTA)$_2$], probably produced during the mass fragmentation, was also observed (Table 3, entries 2 and 6).
36 Previous work suggests guanine nitrogen-7 as a preferential target for ruthenium(II) complexes, even when many ruthenium(II) complexes does not react selectively with nucleobases.S. Parsons, R. A. Coxall, R. O. Gould and P. J. Sadler, *J. Am. Chem. Soc.*, 2002, **124**, 3064–3082.
37 H. Chen, J. A. Parkinson, R. E. Morris and P. J. Sadler, *J. Am. Chem. Soc.*, 2003, **125**, 173–186.
38 H. K. Liu, S. J. Berners-Price, F. Wang, J. A. Parkinson, J. Bella and P. J. Sadler, *Angew. Chem., Int. Ed.*, 2006, **45**, 8153–8156.
39 O. Novakova, H. Chen, O. Vrana, A. Rodger, P. J. Sadler and V. Brabec, *Biochemistry*, 2003, **42**, 11544–11554.
40 C. S. Allardyce, P. J. Dyson, D. J. Ellis and S. L. Heath, *Chem. Commun.*, 2001, 1396–1397.
41 C. Scolaro, A. Bergamo, L. Brecacin, R. Delfino, M. Cocchietto, G. Laurenczy, T. J. Geldbach, G. Sava and P. J. Dyson, *J. Med. Chem.*, 2005, **48**, 4161–4171.
42 W. H. Ang, E. Daldini, C. Scolaro, R. Scopelliti, L. Juillerat-Jeannerat and P. J. Dyson, *Inorg. Chem.*, 2006, **45**, 9006–9013.
43 S. P. Newman, M. P. Leese, A. Purohit, D. R. James, C. E. Rennie, B. V. Potter and M. J. Reed, *Int. J. Cancer*, 2004, **109**, 533–540.
44 F. Mollinedo, C. Gajate, A. I. Morales, E. del Canto-Janez, N. Justies, F. Collia, J. V. Rivas, M. Modolell and A. Iglesias, *J. Pharmacol. Exp. Ther.*, 2009, **329**, 439–449.
45 M.-H. David-Cordonnier, C. Gajate, O. Olmea, W. Laine, J. de la Iglesia-Vicente, C. Perez, C. Cuevas, G. Otero, I. Manzanares, C. Bailly and F. Mollinedo, *Chem. Biol.*, 2005, **12**, 1201–1210.
46 Bruker 2004. *Collect data collection software*. Bruker AXS, Delft, The Netherlands.
47 Z. Otwinowski and W. Minor, *Methods Enzymol.*, 1997, **276**, 307–326.
48 R. H. Blessing, *Acta Crystallogr., Sect. A: Found. Crystallogr.*, 1995, **51**, 33–38.
49 L. J. Farrugia, *J. Appl. Crystallogr.*, 1999, **32**, 837–838.

50 P. T. Beurskens, G. Admiraal, G. Beurskens, W. P. Bosman, S. García-Granda, R. O. Gould, J. M. M. Smits, C. Smykalla, *The DIRDIF Program System; Technical Report of the Crystallographic Laboratory*University of Nijimegen: Nijimegen, The Netherlands, 1999.
51 G. M. Sheldrick, SHELXL-97, *Program for the Refinement of Crystal Structures*, University of Göttingen, 1997.
52 *International Tables for X-Ray Crystallography, Vol. IV*, Birmingham, Kynoch Press. (Present distributor: Kluwer Academic Publishers, Dordrecht), 1974.
53 M. Nardelli, *Comput. Chem.*, 1983, **7**, 95–98.
54 A. L. Spek, *PLATON, a multipurpose crystallographic tool*, Utrecht University, Utrecht, The Netherlands, 2007.

